doi:10.4149/neo_2021_210318N358

microRNA-375 inhibits the malignant behaviors of hepatic carcinoma cells by targeting NCAPG2

Hai-Tao DAI[1,#], Shu-Tong WANG[2,#], Bin CHEN[3], Ke-Yu TANG[3], Nan LI[1], Chun-Yong WEN[3], Yuan WAN[3], Gui-Yuan ZHANG[3], Yong-Hui HUANG[3,*], Zhi-Jun GENG[4,5,*]

[1]Department of Radiology, The First Affiliated Hospital, Sun Yat-sen University, Guangzhou, Guangdong, China; [2]Department of Hepatic Surgery, The First Affiliated Hospital, Sun Yat-sen University, Guangzhou, Guangdong, China; [3]Department of Interventional Radiology, The First Affiliated Hospital, Sun Yat-sen University, Guangzhou, Guangdong, China; [4]State Key Laboratory of Oncology in South China, Collaborative Innovation Center for Cancer Medicine, Sun Yat-sen University Cancer Center, Guangzhou, Guangdong, China; [5]Department of Radiology, Sun Yat-sen University Cancer Center, Guangzhou, Guangdong, China

**Correspondence: hyongh@mail.sysu.edu.cn; gengzhj@sysucc.org.cn*
[#]Contributed equally to this work.

Received March 18, 2021 / Accepted August 2, 2021

Hepatocellular carcinoma (HCC) is a major cause of cancer-related deaths worldwide. Emerging evidence has revealed the vital functions of microRNAs (miRNAs) in cancer malignant progressions. miR-375 has been verified to serve as an antioncogene in tumorigenesis and a potential therapeutic target in various types of cancer. In this study, we aimed to determine the role of miR-375 in the regulation of chemoresistance and metastasis of HCC. Differentially expressed miR-375 and NCAPG2 were externally validated using expression data from The Cancer Genome Atlas (TCGA) database. Quantitative real-time polymerase chain reaction (qRT-PCR) was performed to detect the expression levels of miR-375 in HCC tissues and cell lines. miR-375 mimics and NCAPG2-overexpression were transfected into HepG2 and Huh7 cells to establish miR-375 overexpression models. Cell Counting Kit-8, Transwell, and flow cytometry experiments were conducted to monitor cell proliferation, migration, and apoptosis. The targeting relationship between miR-375 and non-SMC condensin II complex subunit G 2 (NCAPG2) was determined by qRT-PCR, western blot, and luciferase reporter gene assay. Kyoto Encyclopedia of Genes and Genomes (KEGG) pathway analyses were conducted using Gene Set Enrichment Analysis (GSEA). The pathway enrichment analysis was used to predict the potential pathways for further study. miR-375 was significantly downregulated in HCC tissues and cells compared to adjacent tissue and normal hepatocyte cell line respectively while NCAPG2 was upregulated. The targeting relationship was verified by luciferase reporting assay, and miR-375 could target the 3'UTR of NCAPG2 mRNA and effectively suppress NCAPG2 protein expression. Replenishing of miR-375 significantly repressed HCC cell proliferation and migration, and induced cell apoptosis. Overexpression of NCAPG2 recovered those biological abilities in miR-375 overexpressed cells. Collective data suggested that miR-375 served as a tumor suppressor via regulating NCAPG2. Replenishing of miR-375 or knockout of NCAPG2 could be therapeutically exploited for HCC.

Key words: hepatocellular carcinoma, microRNA-375, non-SMC condensin I complex subunit G 2, proliferation, apoptosis

Liver cancer is the fifth most frequent cancer worldwide and the second common cause of cancer-related deaths worldwide, among which hepatocellular carcinoma (HCC) is the most common pathological type [1, 2], especially in China with about 50% of newly diagnosed HCC cases and deaths worldwide [3]. The rates of HCC incidence and mortality have increased across most countries over the past three decades since the primary risk factor of HCC is liver cirrhosis secondary to persistent infection with hepatitis B virus (HBV) or hepatitis C virus (HCV), or alcohol consumption [4]. Large numbers of studies have thoroughly described not only the complex pathogenesis of HCC development and metastasis but also the multiple treatments [5], including the prognosis of HCC patients [4]. Despite improvements in HCC therapy in the past 10 years, the prognosis of HCC patients is usually very poor due to a high incidence of recurrence. An improved understanding of the pathogenesis of HCC development would facilitate the development of more effective outcomes for the diagnosis and treatment of HCC at earlier stages.

Mature miRNAs are a class of non-coding single-stranded RNA molecules of 20–23 nucleotide (nt) in length that control multiple genes expression in many cellular processes. miRNAs are found to adjust target mRNAs' expression by binding

3-untranslated region (UTR) of target mRNAs, thereby reducing stability or translation of mRNA [6]. Additionally, miRNAs also participate in most cellular functions, such as proliferation, apoptosis, differentiation, and metastasis [7, 8]. miRNAs act as remarkable factors in carcinogenesis and receives increasing attention as new non-invasive cancer biomarkers as their aberrant expression and dysregulation can affect the biological processes of cancer cell greatly [9]. Due to their unique maladjusted features throughout tumor progression, accumulating evidence has demonstrated that miRNAs regulate post-transcriptional progressions of HCC by acting as tumor suppressors or oncogenes [10]. For instance, the expression of tumor suppressor miR-122, a liver-specific anti-proliferative miRNA, is usually downregulated in HCC cells compared with that in normal hepatocytes surrounding the tumor [11]. miR-887 has been proved to promote the tumorigenesis of HCC via targeting von Hippel-Lindau tumor suppressor [12]. Besides, serum miRNA-27a and miRNA-18b as potential predictive biomarkers of hepatitis C virus-associated HCC [13]. Among tumor-associated miRNAs, miR-375 has been studied in multiple cancers including osteosarcoma, gastric cancer (GC), prostate cancer (PC), oral squamous cell carcinoma (OSCC), and glioblastoma (GBM) [14–17]. Despite these studies of miR-375 in different cancers, the functions and downstream mechanism of miR-375 in HCC remain largely unknown.

Non-SMC condensin II complex subunit G2 (NCAPG2) belongs to the chromosome condensin II complex, which plays essential roles in mitotic chromosome assembly and segregation [18]. Both condensins contain 2 invariant structural maintenance of chromosome (SMC) subunits, SMC2 and SMC4, which contain different sets of non-SMC subunits. NCAPG2 is 1 of 3 non-SMC subunits that define condensin II. Altered expression of NCAPG2 has been the focus in the study of different cancers, including lung adenocarcinoma [19], glioblastoma [20], and HCC [21]. Although there are numerous studies of the effects of NCAPG2 on tumor progression, information about the effects of NCAPG2 on HCC is still very sparse, and the exact mechanism of action of NCAPG2 remains unclear. The present study aimed to resolve this issue.

This study was undertaken to clarify how miR-375 regulates HCC progression by affecting the PI3K/AKT pathway and NCAPG2. miR-375 expression in HCC tissues and cell lines was analyzed to reveal the role of miR-375 in the progression of HCC. Additionally, the effects of miR-375 on the proliferation and apoptosis of HCC cells and its potential downstream targets were explored.

Materials and methods

Bioinformatics analysis. Clinical data for patients with HCC were obtained from The Cancer Genome Atlas (TCGA) database (https://tcga-data.nci.nih.gov; https://gdac.broadinstitute.org/) available to the public. miRNAs and mRNAs with differential expressions in HCC tissues were analyzed. The Kaplan-Meier curve was used to test lncRNA association with time to progression. All TCGA data are now available without restrictions on their use in publications or presentations.

Ethical statement. The use of clinical samples was approved by the Ethics Committee of the First Affiliated Hospital, Sun Yat-Sen University according to the Declarations of Helsinki. Written informed consent was obtained and signed by each patient enrolled in the present study.

Tissue samples. A total of 131 pairs of HCC tissues were collected from patients who received surgery from the Department of the First Affiliated Hospital, Sun Yat-sen University between January 2010 and January 2019. None of the HCC patients had received adjuvant radiotherapy or chemotherapy before surgery. Tissues were stored in liquid nitrogen at –80 °C for follow-up testing.

Cell lines. Human HCC cell lines (HepG2, Hep3B, and Huh7) and human hepatocyte immortalized cell line (THLE-3) were purchased from the Institute of Biochemistry and Cell Biology of the Chinese Academy of Sciences (Shanghai, China). All cells were cultured in Dulbecco's modified Eagle's medium (DMEM; Gibco; Thermo Fisher Scientific, Inc.) containing 10% fetal bovine serum (FBS; Gibco) and 1% v/v penicillin/streptomycin solution (Sigma-Aldrich), and incubated in the incubator with 5% CO_2 at 37 °C. The medium was replaced every 3 days. Cells in the logarithmic growth phase were used for experiments.

RNA isolation and RT-qPCR analysis. The total RNA was extracted using TRIzol reagent (Thermo Fisher Scientific, Inc.) and cDNA was synthesized, using the iScript™ cDNA reverse transcription kit (Biorad, China). To examine the miR-375 expression, RT-qPCR was conducted using the PrimeScript® miRNA RT-PCR Kit (Takara, Dalian, China) on a 7900HT Real-Time PCR System (Applied Biosystems). To examine the expression of NCAPG2, RT-qPCR was performed using SYBR-Green PCR kit (Invitrogen) following the manufacturer's procedure. U6 was used to normalize miR-375 while GAPDH was used to normalize NCAPG2 mRNA. The relative expression levels of miR-375 and NCAPG2 were calculated using the $2^{-\Delta\Delta ct}$ method. The primers sequences of the evaluated genes are shown in Table 1. All experiments were repeated at least three times.

Cell transfection. When cells reached 80% confluence, miR-375 mimics and mimics negative controls (Control), pCDNA3.1-NCAPG2 (NCAPG2) synthesized by GenePharma (Shanghai, China), were transfected into cells using Lipofectamine 2000 (Invitrogen) according to the manufacturer's procedure. The cells were harvested 48 h after transfection for follow-up tests. Transfection efficiency was measured by RT-qPCR.

Cell Counting Kit-8 Assay. Cell Counting Kit-8 (CCK-8) assay was carried out according to the instructions of the CCK-8 kit and cell proliferation was detected. Cells were harvested in the logarithmic phase, digested with trypsin

(0.25%), and the cell suspension was prepared with 10% FBS. HepG2 and Huh7 cells (3×10^3 cells/well) were cultured in 96-well plates for 1, 2, 3, 4, and 5 days, respectively. Then, cells were incubated with 10 µl of the CCK-8 solution (Beyotime) at 37 °C for 1 h. The culture was continued at 37 °C for 2 h and then terminated. The empty control wells were zeroed. The absorbance value of each well was measured at 450 nm under a microplate reader. The relative OD ratio was used to reflect the cell proliferation capacity. The average value of five wells in each group was taken. Every experiment was repeated three times.

Transwell assay. Cells were transfected with control and miR-375 mimics for 24 h. Cell migration was assessed with a Transwell membrane filter insert (8 µm pore size). Briefly, the upper chamber was incubated with 200 µl serum-free 3×10^4 cell suspension and the lower chamber was filled with 500 µl DMEM culture medium containing 10% FBS. Cells were then incubated in a humidified 5% CO_2 incubator at 37 °C for 24 h. Cells on the upper layer of the membrane were removed with a cotton swab and those migrated cells in the lower chamber through the membrane were fixed in 4% paraformaldehyde for 5 min and stained with 0.3% crystal violet dye for 10 min. At least five fields of each membrane were observed and photographed under a microscope. The number of cells was presented as the average number of cells in every microscopic field of every well. Each experiment was repeated at least three times.

Apoptosis analysis. After 48 h of incubation, transfected cells were digested by trypsin and centrifuged at 1000× g. The sedimentary cells were resuspended and adjusted at the density of 1×10^6 cells/ml. The cell suspension was incubated in a dark room for 15 min after the addition of 5 µl Annexin-V-APC and 5 µl PI solutions. Then, the flow cytometer was used to analyze the cell apoptosis using CellQuest (Easycyte plus; Millipore, France).

Xenograft model. All animal procedures were approved by the Institutional Animal Care and Use Committee of the First Affiliated Hospital, Sun Yat-Sen University. Xenograft model in female BALB/c nude mice was formulated by subcutaneous injection of 0.2 ml exponentially growing lentivirus infected HepG2 cell suspensions at a density of 2×10^7 cell/ml. When the mice were euthanized, tumor weight was measured. Tumor growth was assessed using a caliper and tumor volumes (V) were estimated as $V=\pi/6\times L\times W\times W$ (L and W was tumor length and width, respectively) at day 10, 14, 17, 21, and 23 post tumor inoculation. Mice were purchased from Shanghai Lingchang Experimental Animals Co., Ltd. Mice were sacrificed and the tumor tissues were removed for Ki-67 immunostaining.

Ki67 staining assay. Tissue slides were blocked with 3% PBS-H_2O_2 and were incubated with primary antibody Ki67 (ab16667, 1:200, Abcam) at 4 °C overnight. Then, the slides were incubated with HRP goat anti-rabbit IgG at room temperature for 2 h. Finally, all slides were stained by Hematoxylin (# BA4041, Baso) and Eosin (# BA4022, Baso).

miRNA target prediction and Dual-Luciferase Reporter Assay. TargetScanHuman 7.2 (http://www.targetscan.org/) and miRcode (http://www.mircode.org/) were used to predict the target genes of miR-375 and found the binding region (chr7:158433540-158433561[–]) on NCAPG2. Cells were seeded in a 24-well plate. The segments of NCAPG2-3'UTR-WT (wild type) or NCAPG2-3'UTR-MUT (mutant) were constructed and then inserted into the luciferase reporter assay vector pmirGLO (Promega, USA). Cells were harvested 48 h after co-transfection with miR-375 mimics or control (50 nmol/l) (GenePharma, Shanghai, China), and WT or MUT of NCAPG2 (500 ng) using Lipotectamine™ 2000 (Invitrogen). The luciferase activity was measured using the Dual-Luciferase Reporter Assay System (Promega, USA). Firefly luciferase activity was normalized to *Renilla* luciferase activity. Each experiment was conducted in triplicate and repeated three times.

Gene set enrichment analysis (GSEA). Gene Set Enrichment Analysis (GSEA) (http://software.broadinstitute.org/gsea) was conducted based on the pathway gene set Kyoto Encyclopedia of Genes and Genomes (KEGG) (https://www.kegg.jp/kegg/), which were used to implement gene set enrichment analysis. The expression data of total normalized mRNAs were uploaded to the GSEA v3.0 software. The default weighted enrichment statistic was adopted to process the data 1000 times, with normalized $p<0.05$ considered to be significantly enriched. Next, the highest up- and down-regulated results of the GSEA reports were selected to undergo graphics processing using the "ggplot2" package in R. Dotplot was also used to visualize the data from the GSEA and illustrate the distribution of multiple pathways. The data of miRNA involved in pathways was from KEGG.

Western blot. Cells were lysed with a Cell Lysis Reagent (Sigma-Aldrich) for total protein extraction. The protein concentration was determined with a BCA protein assay kit (Beyotime, Shanghai, China). Total protein (45 µg) was boiled for 5 min in 1× loading buffer, chilled on ice, and then separated by 10% sulfate sodium salt-polyacrylamide gel electrophoresis (SDS-PAGE) and transferred onto a polyvi-

Table 1. Specific primer sequences for qRT-PCR.

	Forward primer sequences (5'->3')	Reverse primer sequences (5'->3')
miR-375	GTGCAGGGTCCGAGGT	AGCCGTTTGTTCGTTCGGCT
NCAPG2	AAGTGAGAACTACGAAGCCCT	CCCACCAGGTAACACACAAATC
U6	CTCGCTTCGGCAGCACA	AACGCTTCACGAATTTGCGT
GAPDH	GTTCGACAGTCAGCCGCATC	GGAATTTGCCATGGGTGGA

nylidene fluoride (PVDF) membrane (Merck Millipore, USA). Membranes were blocked with 5% skim milk powder for 2 h. After washing, the primary antibodies for NCAPG2 (ab70350, 1:5000, Abcam), cleaved-Caspase3 (ab2302, 1:100, Abcam), Caspase3 (ab49822, 1:500, Abcam), AKT (ab8805, 1:500, Abcam), and p-AKT (ab38449, 1:1000, Abcam) were added and incubated overnight at 4 °C. The horseradish peroxidase (HRP)-conjugated secondary antibodies at a 1: 2000 dilution were then used to incubate the membranes for 1 h. The targeting proteins on the membrane were visualized with enhanced chemiluminescence (ECL) detection system. GAPDH (ab181602, 1:10000, Abcam) was used as an internal control and the experiments were repeated three times.

Statistics processing. Quantitative data were expressed as the mean ± standard deviation (SD), and GraphPad Prism 8.0 software was used for statistical analysis. Differences between two groups were identified by unpaired t-tests, and one-way analysis of variance (ANOVA) was used to identify differences between three or more groups. All experiments were repeated at least three times. A p-value <0.05 indicates the comparison is statistically significant.

Results

Expression of miR-375 was downregulated in HCC tissues and predicts poor prognosis. Microarray analysis based on the TCGA database set was used to identify differentially expressed miRNA in HCC tissues and normal tissues. As shown in Figure 1A, miR-375 had been reported to act as tumor suppressor molecular in multiple tumors and it was significantly downregulated in the HCC patients, predicting its expression and biological function in HCC tumorigenesis. It is worth mentioning that overall survival (OS) rates of patients with HCC with highly expressed miR-375 were higher than those with low expression of miR-375 (p=0.0039, Figure 1B). What is more, we further analyzed the relationship between miR-375 and the clinicopathological characteristics of HCC patients (Table 2). We found that in patients the low expression miR-375 was related to high T infiltrate and T stages. The data indicated that miR-375 might play a tumor-suppressing role in HCC, as well as showed that miR-375 was a potential biomarker for the clinical outcome of patients with HCC.

miR-375 suppressed the proliferation, migration, and induced apoptosis of HCC cells. To explore the effects of miR-375 on HCC, we first detected the expression profile of miR-375 in HCC cells. As shown in Figure 1D, miR-375 expression dramatically decreased in three HCC cell lines (HepG2, Hep3B, and Huh7) when compared with the normal hepatocyte immortalized cell line (THLE-3) (Figure 2A). Inspired by the above data, HepG2 and Huh7 cells were then selected for subsequent experiments. Further, miR-375 was overexpressed by transfecting miR-375 mimics into HepG2 and Huh7 cells. The transfection efficiency was analyzed using an RT-qPCR assay (Figure 2B). Subsequently, it was observed that upregulation of miR-375 significantly

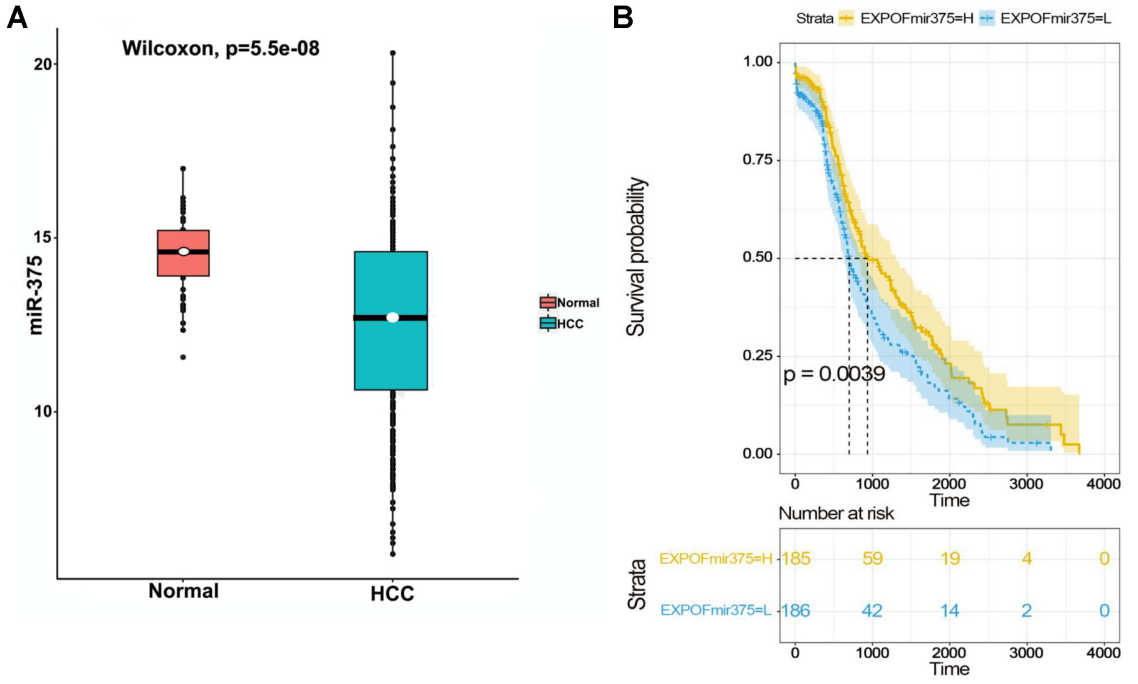

Figure 1. Downregulation of miR-375 predicts a worse prognosis in patients with HCC. A) The expression of miR-375 was downregulated in HCC tissues from the TCGA dataset. B) Differences in overall survival rate (OS) between HCC patients with miR-375 expression were analyzed by Kaplan-Meier analysis. The patients with high miR-375 expression exhibited a higher overall survival rate. miR-microRNA; HCC-hepatocellular carcinoma.

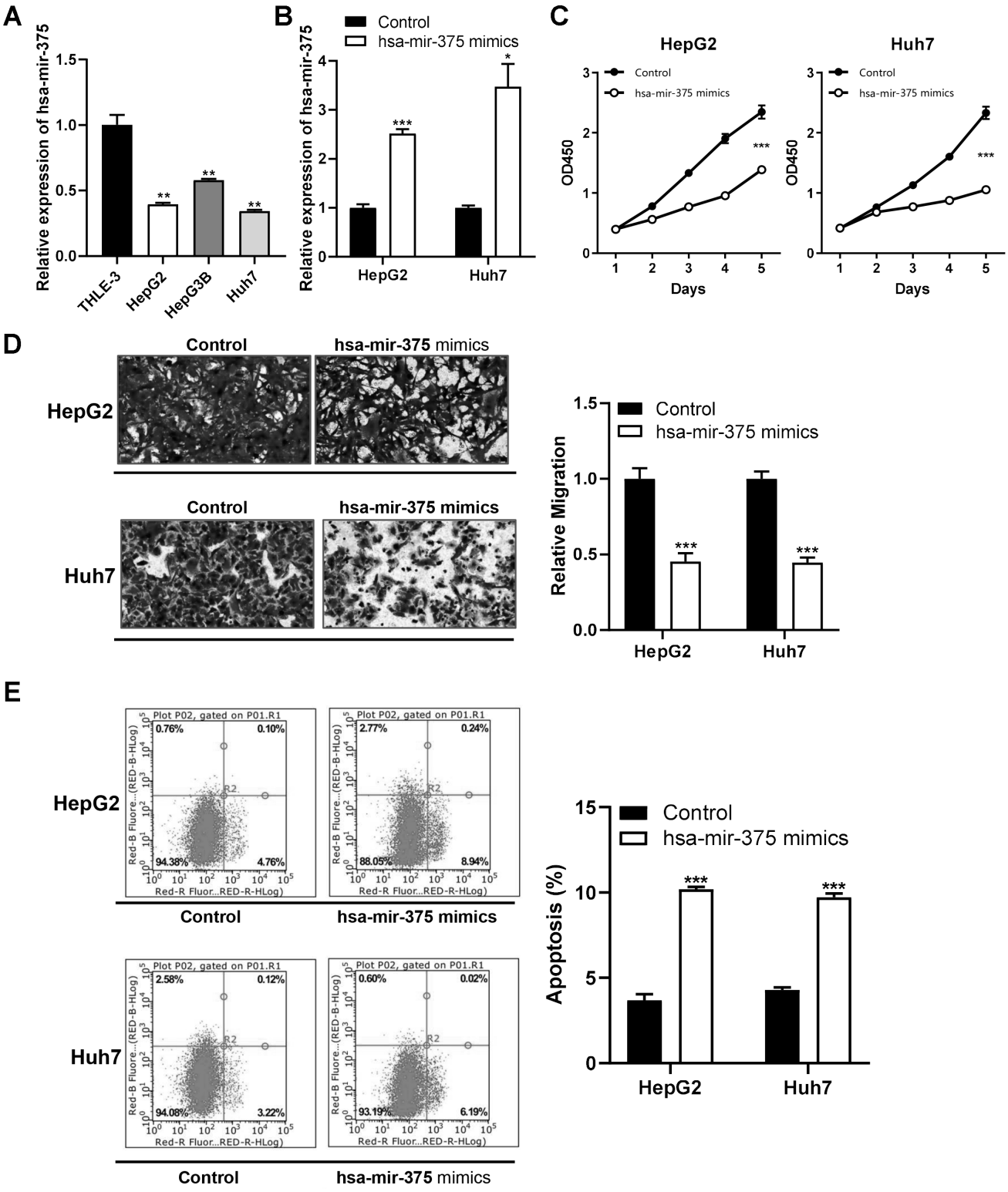

Figure 2. miR-375 inhibited cell proliferation, migration, and promoted cell apoptosis in HCC cells. A) miR-375 expression in HCC cell lines, including HepG2, Huh7, and Hep3B, and in the immortalized normal liver THLE-3 cell line was measured by RT-qPCR. B) Transfection of miR-375 mimics increased miR-375 expression in HepG2 and Huh7 cells. C) The CCK-8 assay revealed that overexpressed miR-375 can suppress the proliferation of HepG2 and Huh7 cells. D) Transwell assay indicated that the overexpression of miR-375 significantly impeded the migration of HepG2 and Huh7. E) Flow cytometry demonstrated that the apoptosis of HepG2 and Huh7 was elevated after the overexpression of miR-375. *p<0.05, **p<0.01, ***p<0.001

decreased cell proliferation (Figure 2C) and migration (Figure 2D) in HepG2 and Huh7 cells. Besides, the overexpression of miR-375 significantly promoted cell apoptosis (Figure 2E) in HepG2 and Huh7 cells. This result indicated that miR-375 might be associated with tumor metastasis and survival in HCC.

Overexpression of miR-375 suppressed HCC *in vivo*. To further verify the cancer-suppressing effect of miR-375 in HCC, we conducted a tumor-forming experiment in nude mice. The results showed that the tumor volume and weight in the overexpressed miR-375 group were significantly lower than those in the control group (Figures 3A–3C). Moreover, Ki67 staining was used to detect the proliferative activity of tumors, which was shown to be significantly weaker in the miR-375 mimic group than the control group (Figure 3D).

miR-375 targeted the 3'UTR region of NCAPG2. As mentioned above, the prediction by TargetScanHuman and miRcode suggested that NCAPG2 might be the target of miR-375, and it was predicted the NCAPG2 sequence that could potentially bind with miR-375 (Figure 4A). The luciferase reporter gene assay was performed to verify their binding relationship. The result revealed that the luciferase activity of cells co-transfected with miR-375 mimics and 3'UTR-WT of NCAPG2 was significantly lower than that of cells co-transfected with NC and 3'UTR-WT of NCAPG2 (Figure 4B), whereas miR-375 mimics had no effect on the fluorescence of the MUT recombinant plasmid (Figure 4B). Meanwhile, miR-375 mimics could inhibit the expression of NCAPG2 both at mRNA and protein levels (Figures 4C, 4D). Taken together, these results revealed that miR-375 directly targeted the 3'UTR of NCAPG2 in HCC cells and inhibited NCAPG2 expression in HCC.

Interestingly, Pearson's correlation analysis indicated that there was a negative correlation between NCAPG2 expression and miR-375 expression in HCC tissues (Figure 4E). Additionally, NCAPG2 was significantly upregulated in the

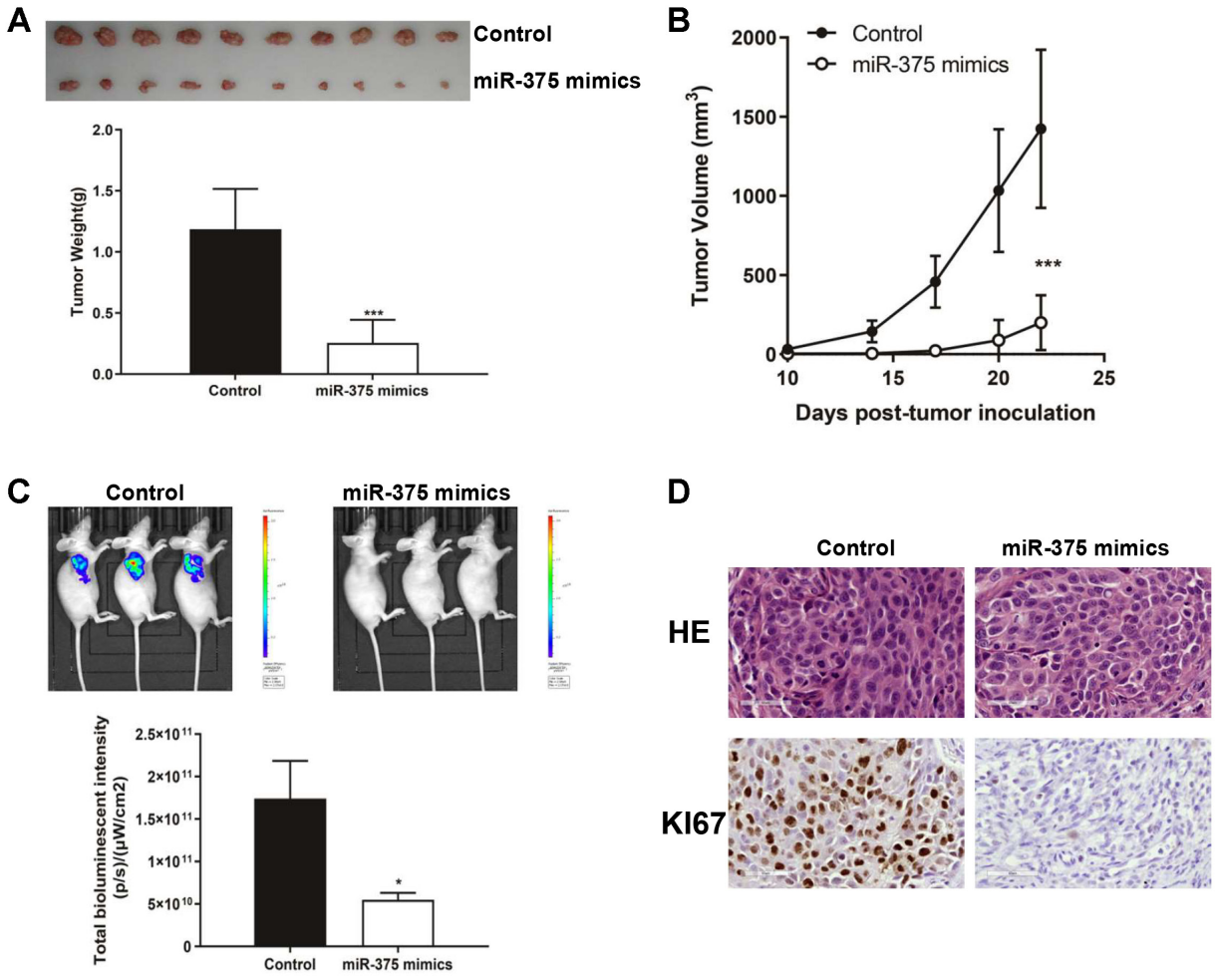

Figure 3. Highly expressed miR-375 can suppress the progression of hepatocellular carcinoma (HCC). A, B) Mice tumor images, weight changes (A), and tumor volume growth curves (B) for subcutaneous xenografts. Images were taken by camera (respectively). n=10, ***p<0.001; C) Images of the subcutaneous xenografts from the miR-375 mimics and control groups. Images were taken by Perkin Elmer IVIS Spectrum (respectively). n=10, *p<0.05; D) Representative images of sections sliced from the indicated tumors and H&E (above) and Ki67 (below) staining, respectively (scale bar = 50 μm)

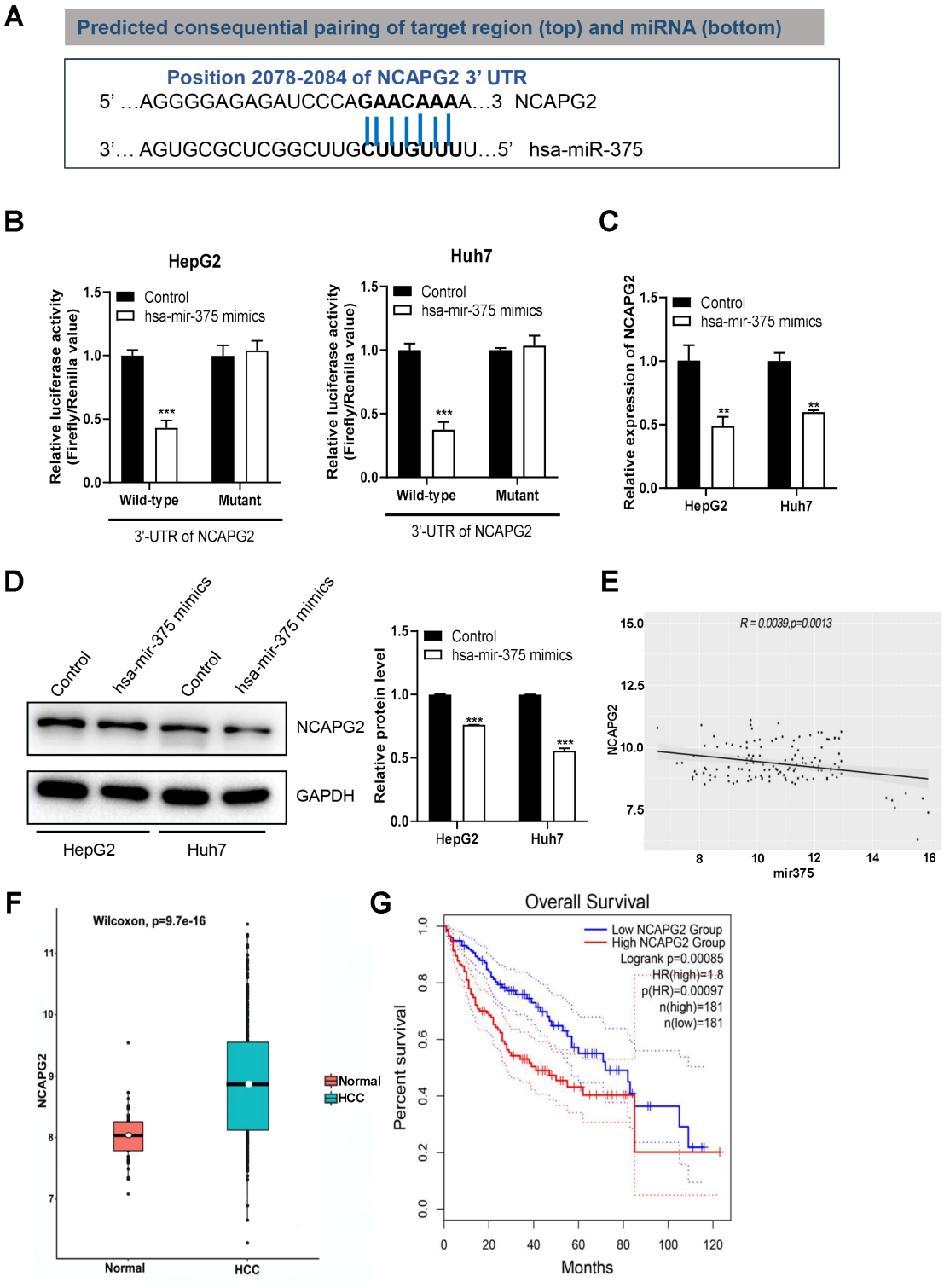

Figure 4. NCAPG2 was a target of miR-375 in hepatocellular carcinoma. A) Putative miR-375 binding sequence in the 3'-UTR of NCAPG2 predicted using the Target Scan Human. B) Relative luciferase activity of HepG2 and Huh7 cells co-transfected with miR-375 mimics with wild-type or mutant 3'-UTR of NCAPG2. C, D) NCAPG2 expression was detected by (C) reverse transcription-quantitative PCR and (D) western blot analysis after transfection with miR-375 mimics. E) Correlation between the expression levels of miR-375 and NCAPG2 analyzed by Spearman's correlation test. F) The expression of NCAPG2 was upregulated in HCC tissues from the TCGA dataset. G) Differences in overall survival rate (OS) between HCC patients with NCAPG2 expression were analyzed by Kaplan-Meier analysis. The patients with high NCAPG2 expression exhibited a lower overall survival rate. **p<0.01, ***p<0.001. Abbreviations: miR-microRNA; HCC-hepatocellular carcinoma

Table 2. Relationship between miR-375 or NCAPG2 expression and clinical characteristics of patients with hepatocellular carcinoma.

Features	No. of patients	miR-375 expression		p-value	NCAPG2 expression		p-value
		low	high		low	high	
All patients	131	70	61		64	67	
Age (years)				0.34			0.434
≤64	66	38	28		30	36	
>64	65	32	33		34	31	
Gender				0.382			0.536
Male	95	53	42		48	47	
Female	36	17	19		16	20	
T Infiltrate				0.402			0.002*
T1	49	26	23		28	21	
T2	39	17	22		26	13	
T3	35	18	17		8	27	
T4	8	3	5		2	6	
Stage				0.000***			0.000**
1	25	1	24		20	5	
2	41	13	28		22	19	
3	54	52	2		17	37	
BMI				0.27			0.463
≤24.13	59	35	24		31	28	
>24.13	59	29	30		27	32	
Weight				0.933			0.417
<69 kg	60	32	28		31	29	
≥69 kg	61	33	28		27	34	

Notes: *p<0.05, **p<0.01, ***p<0.001

HCC patients (Figure 4F), and the OS time of HCC patients with high expression of NCAPG2 was significantly shorter than those with low expression of NCAPG2 (p=0.00085, Figure 4G). We also found that patients expressing high NCAPG2 are related to high T Infiltrate and T stages (Table 2). The data indicated that NCAPG2 might play a tumor-promoting role in HCC.

NCAPG2 overexpression reversed the inhibitory effect of miR-375 in HCC cells. To confirm the involvement of NCAPG2 in the anticancer activity of miR-375 in HCC cell lines, HepG2 and Huh7 cells were transfected with the pcDNA-NCAPG2 plasmid. The results of both qRT-PCR and western blotting showed that the expression of NCAPG2 was significantly in the NCAPG2 group (Figures 5A, 5B), suggesting that the overexpression of NCAPG2 (NCAPG2 pcDNA) was successfully obtained. Importantly, functional analysis revealed that overexpression of NCAPG2 significantly attenuated the inhibitory effect of miR-375 mimics on the proliferation and apoptosis of HepG2 and Huh7 cells (Figures 5C, 5D). Simultaneously, western blot indicated miR-375 could elevate the expression of apoptosis-related protein cleaved-Caspase3 while NCAPG2 had the opposite effect (Figure 5E). The present results suggest that the tumor-suppressive role of miR-375 in HCC is partially mediated by NCAPG2 downregulation and miR-375 the malignant behaviors of hepatic carcinoma cells by directly targeting NCAPG2.

Enrichment of related pathways of miR-375/NCAPG2 in HCC cells. To confirm the downstream-associated molecular mechanisms underlying the miR-375 axis in HCC cells, the enrichment analysis of related-pathway was performed using GSEA. KEGG enrichment analysis of differentially expressed genes when miR-375 was silenced in HCC cells showed that miR-375 might be involved in the regulation of the PI3K-AKT signaling pathway. According to the enrichment score from the GSEA report, the pathways involved in HCC cells were screened out when miR-375 was downexpressed. Based on the adjusted p-value of each pathway, the distributions of the top 8 or 10 scored KEGG pathways were drawn in dotplots (Figure 6A). The GSEA enrichment plot showed that most genes involved in the PI3K-AKT signaling pathway were found in the region where miR-375 was downregulated in HCC cells (Figure 6B). Both dotplot and GSEA enrichment plot showed that the PI3K-AKT pathway was one of the most significantly activated pathways in HCC cells. Western blot also showed that miR-375 mimic remarkably reduced p-AKT expression in HepG2 and Huh7 cells (Figure 6C). Furthermore, reintroduction of NCAPG2 could weaken the inhibition of miR-375 on the PI3K-AKT signaling pathway by upregulating p-AKT expression in HCC cells (Figure 6C), which demonstrated the importance of NCAPG2 in miR-375 regulating PI3K/AKT. Combining these bioinformatics results, we speculated that the PI3K-AKT signaling pathway could influence the functions of miR-375 targeting NCAPG2, thereby participating in HCC progression.

Discussion

Hepatocellular carcinoma is a highly fatal malignant cancer worldwide, with an annual mortality of about 700,000 persons globally [22]. Elucidating the underlying molecular mechanism of HCC progression is critical for the identification of new therapeutic targets for HCC. Due to the current status of the treatment and diagnosis of HCC is not optimistic, numerous clinical trials searching for a more ideal tool are running. One of these tools are the miRNAs, which can be considered as a promising diagnostic as well as a prognostic tool for HCC. The importance of dysregulation and expression of miRNAs has been confirmed in many cancers. Abnormal expression of miRNAs is related to tumorigenesis of HCC and the plasma miRNA expression has also been investigated as a possible marker of HCC [22–24]. Additionally, miRNAs have a potential prognostic impact in patients with HCC [1]. In our study, we used public TCGA databases to find that miR-375 is significantly downregulated in liver hepatocellular carcinoma (LIHC) tissues. Additionally, we provide direct evidence that the modulation of miR-375 greatly influenced the propensity of HCC cells to migrate and apoptosis. Indeed, the restora-

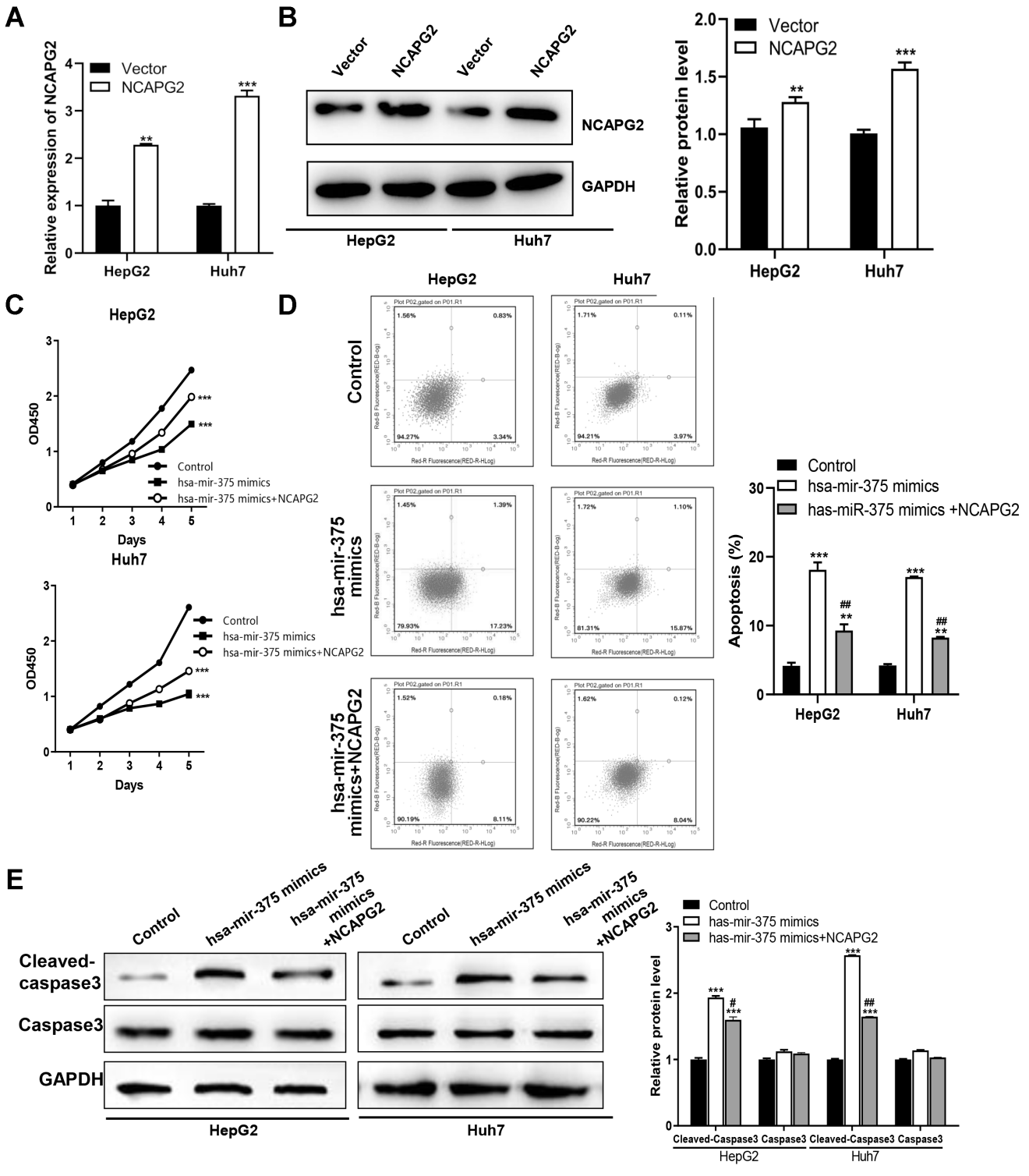

Figure 5. Overexpression of NCAPG2 reversed the suppressive effect of miR-375 on the proliferation and apoptosis of hepatocellular carcinoma cells. HepG2 and Huh7 cells were transfected with pcDNA-vector or pcDNA-NCAPG2, and the overexpression of NCAPG2 was confirmed by A) reverse transcription-quantitative PCR and B) western blot analysis. C) Proliferation of HepG2 and Huh7 cells detected by a Cell Counting Kit-8 assay following transfection of miR-375 mimics and NCAPG2. D) Apoptosis of HepG2 and Huh7 cells determined by flow cytometry after transfection with miR-375 mimics and NCAPG2. E) Relative expression of cleaved-caspase3 and caspase3 in HepG2 and Huh7 cells co-transfected with miR-375 mimics and/or NCAPG2 was detected by western blot. **p<0.01, ***p<0.001 vs. control; ##p<0.01, ###p<0.001 vs. miR-375 mimics

tion of miR-375 resulted in the deletion of proliferation and migrating properties as well as emancipated cell apoptosis in HCC cells. Similar findings have been confirmed by previous experiments that miR-375 has been reported to be significantly dysregulated in many cancers as a suppressor or oncogene. For instance, inhibition of miR-375 reversed attenuation of cell proliferation, migration, and invasion, and therefore promoted tumorigenesis in osteosarcoma [14]. Wnt5a overexpression significantly reversed miR-375-mediated proliferation, migration, and invasion in GBM

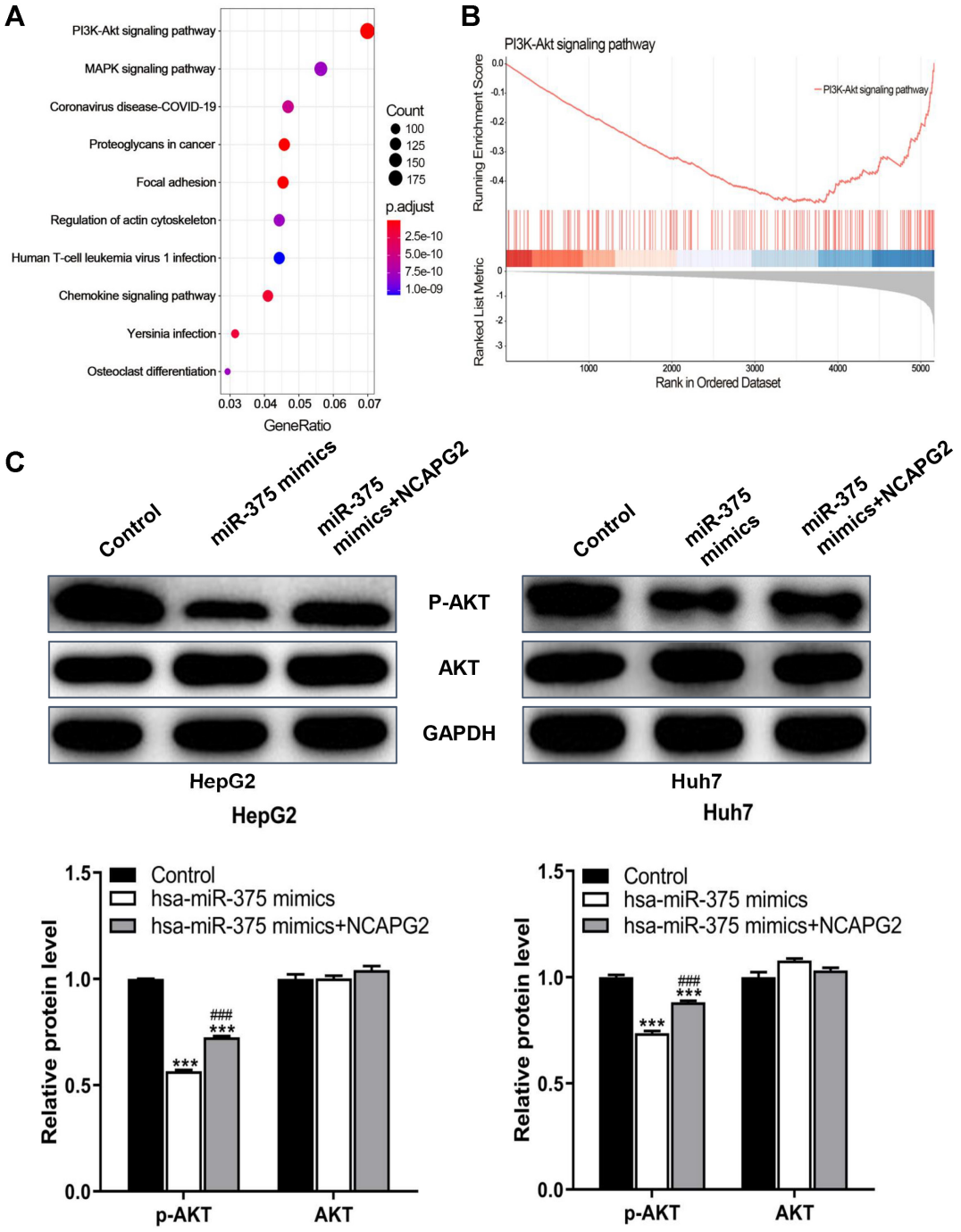

Figure 6. Distributions of several KEGG pathways gene sets in HCC cells. A) Dotplot of GSEA reports showed that the top 10 signaling pathways including the PI3K/Akt signaling pathway were upregulated. B) GSEA report for the PI3K/Akt signaling pathway showed that it was upregulated in miR-375 mimics induced-HCC cells. C) Relative expression of AKT and p-AKT in HepG2 and Huh7 cells co-transfected with miR-375 mimics and/or NCAPG2 was detected by western blot. ***p<0.001 vs. control; ###p<0.001 vs. miR-375 mimics

cells [15]. The results of the TCGA database verified the expression of miR-375 in PC tissues was obviously higher than that in adjacent non-cancerous tissues [16]. Replenishing of miR-375 significantly repressed OSCC cell viability, proliferation, invasion, and migration, and induced cell apoptosis and G1/G0 arrest while the overexpression of SLC7A11 recovered those biological abilities in miR-375 upregulated-cells [17]. Simultaneously, these findings demonstrated that their target genes of miRNAs could negatively regulate miRNA expression and reverse its effect on cancer progressions. In an attempt to identify the underlying molecular mechanisms responsible for the impact of miR-375 on cell motility, we used miRNA target prediction algorithms on genes negatively correlated with miR-375. Interestingly, an evolutionary conserved binding site for miR-375 was detected in the 3'UTR of NCAPG2 mRNA. Therefore, we speculated that NCAPG2 could influence the anti-neoplastic effect of miR-375 in HCC cells.

Previous researches had demonstrated that NCAPG was involved in the pathogenesis of many kinds of cancers, including prostate cancer [25], pediatric glioma cell [26], renal cell carcinoma [27]. A study had identified that NCAPG2 was involved in hepatocellular carcinoma progression as a novel significant stage-specific differentially expressed gene [28]. Here, we first selected miR-375 as a promising research factor through TCGA data analysis from HCC patients and our data showed that high expression of miR-375 was closely linked with the long OS of HCC patients while high NCAPG2 is linked to worse OS in patients with HCC. Interestingly, based on the expression detection from HCC clinical samples, we found a negative correlation between miR-375 and NCAPG2. Furthermore, miR-375 bound the 3'UTR of NCAPG2 and reduced NCAPG2 expression in HCC cells, suggesting that miR-375 targets NCAPG2 and negatively regulates its expression. Interestingly, our results found that the overexpression of NCAPG2 could elevate the proliferation while reducing cell apoptosis of HCC cells transfected with miR-375 mimics. Accordingly, our data indicated that NCAPG2 could recover the biological abilities of miR-375 on the malignant behaviors of HCC cells. Similar to our results, it was demonstrated that NCAPG2 promoted tumor proliferation by regulating the G2/M phase and was associated with poor prognosis in lung adenocarcinoma [19]. Previous studies indicated that NCAPG2 overexpression promoted HCC proliferation, migration, and invasion through activating STAT3 and NF-κB signaling pathways [21]. NCAPG2 facilitates the malignancy of glioblastoma cells and xenograft tumor growth via HBO1 activation by phosphorylation [20]. The present results shed light on the critical involvement of the miR-375/NCAPG2 signaling pathway in hepatocellular carcinoma. Due to the PI3K-AKT pathway being one of the most significantly activated pathways in HCC cells after miR-375 was inhibited, from both dotplot and GSEA enrichment plot analysis, we speculated that the PI3K-AKT signaling pathway could influence the functions of the miR-375/NCAPG2 axis, thereby participating in HCC progression. In future research, a more comprehensive study of the function and mechanism of miR-375 regulating PI3K-AKT signaling pathway in HCC is needed.

In conclusion, we found that miR-375 and NCAPG2 play significant roles in HCC progression. miR-375 inhibited the proliferation and migration, and induced cell apoptosis in HCC via targeting NCAPG2, providing the basis for future research. Further studies should explore the therapeutic potential of miR-375 and identify other genome-wide targets in addition to NCAPG2 underlying miR-375 in HCC.

Acknowledgments: This study was funded by the Basic and Applied Basic Research Foundation of Guangdong Province (2020A1515010920), Guangzhou Science and Technology Plan Project (202002030084), and Science and Technology Planning Project of Guangdong Province of China (2017A020215010).

References

[1] ATTWA MH. Guide for diagnosis and treatment of hepatocellular carcinoma. World J Hepatol 2015; 7: 1632–1651. https://doi.org/10.4254/wjh.v7.i12.1632

[2] MCGLYNN KA, PETRICK JL, EL-SERAG HB. Epidemiology of Hepatocellular Carcinoma. Hepatology 2021; 73: 4–13. https://doi.org/10.1002/hep.31288

[3] TORRE L A, SIEGEL RL, WARD EM, JEMAL A. Global Cancer Incidence and Mortality Rates and Trends-An Update. Cancer Epidemiol Biomarkers Prev 2016; 25: 16–27. https://doi.org/10.1158/1055-9965.EPI-15-0578

[4] FUJIWARA N, FRIEDMAN SL, GOOSSENS N, HOSHIDA Y. Risk factors and prevention of hepatocellular carcinoma in the era of precision medicine. J Hepatol 2018; 68: 526–549. https://doi.org/10.1016/j.jhep.2017.09.016

[5] MARTÍNEZ-CHANTAR ML, AVILA MA, LU SC. Hepatocellular Carcinoma: Updates in Pathogenesis, Detection and Treatment. Cancers (Basel) 2020; 12: 2729. https://doi.org/10.3390/cancers12102729

[6] BARTEL DP. MicroRNAs: Genomics, Biogenesis, Mechanism, and Function. Cell 2004; 116: 281–297. https://doi.org/10.1016/s0092-8674(04)00045-5

[7] HE L, HANNON GJ. MicroRNAs: small RNAs with a big role in gene regulation. Nat Rev Genet 2004; 5: 522–531. https://doi.org/10.1038/nrg1379

[8] PANNI S, LOVERING RC, PORRAS P, ORCHARD S. Non-coding RNA regulatory networks. Biochim Biophys Acta Gene Regul Mech 2020; 1863: 194417. https://doi.org/10.1016/j.bbagrm.2019.194417

[9] BABAEI K, SHAMS S, KEYMORADZADEH A, VAHIDI S, HAMAMI P et al. An insight of microRNAs performance in carcinogenesis and tumorigenesis; an overview of cancer therapy. Life Sci 2020; 240: 117077. https://doi.org/10.1016/j.lfs.2019.117077

[10] MORISHITA A, MASAKI T. miRNA in hepatocellular carcinoma. Hepatol Res 2015; 45: 128–141. https://doi.org/10.1111/hepr.12386

[11] TSAI WC, HSU SD, HSU CS, LAI TC, CHEN SJ et al. MicroRNA-122 plays a critical role in liver homeostasis and hepatocarcinogenesis. J Clin Invest 2012; 122: 2884–2897. https://doi.org/10.1172/JCI63455

[12] ZOU W, CHENG J. MiR-887 Promotes the Progression of Hepatocellular Carcinoma via Targeting VHL. Technol Cancer Res Treat 2020; 19: 1533033820940425. https://doi.org/10.1177/1533033820940425

[13] RASHAD NM, EL-SHAL AS, SHALABY SM, MOHAMED SY. Serum miRNA-27a and miRNA-18b as potential predictive biomarkers of hepatitis C virus-associated hepatocellular carcinoma. Mol Cell Biochem 2018; 447: 125–136. https://doi.org/10.1007/s11010-018-3298-8

[14] LIU G, HUANG K, JIE Z, WU Y, CHEN J et al. CircFAT1 sponges miR-375 to promote the expression of Yes-associated protein 1 in osteosarcoma cells. Mol Cancer 2018; 17: 170. https://doi.org/10.1186/s12943-018-0917-7

[15] LI GF, CHENG YY, LI BJ, ZHANG C, ZHANG XX et al. miR-375 inhibits the proliferation and invasion of glioblastoma by regulating Wnt5a. Neoplasma 2019; 66: 350–356. https://doi.org/10.4149/neo_2018_180714N484

[16] HE S, SHI J, MAO J, LUO X, LIU W et al. The expression of miR-375 in prostate cancer: A study based on GEO, TCGA data and bioinformatics analysis. Pathol Res Pract 2019; 215: 152375. https://doi.org/10.1016/j.prp.2019.03.004

[17] WU Y, SUN X, SONG B, QIU X, ZHAO J. MiR-375/SLC7A11 axis regulates oral squamous cell carcinoma proliferation and invasion. Cancer Med 2017; 6: 1686–1697. https://doi.org/10.1002/cam4.1110

[18] KIM JH, SHIM J, JI MJ, JUNG Y, BONG SM et al. The condensin component NCAPG2 regulates microtubule-kinetochore attachment through recruitment of Polo-like kinase 1 to kinetochores. Nat Commun 2014; 5: 4588. https://doi.org/10.1038/ncomms5588

[19] ZHAN P, XI GM, ZHANG B, WU Y, LIU HB et al. NCAPG2 promotes tumour proliferation by regulating G2/M phase and associates with poor prognosis in lung adenocarcinoma. J Cell Mol Med 2017; 21: 665–676. https://doi.org/10.1111/jcmm.13010

[20] WU J, LI L, JIANG G, ZHAN H, ZHU X et al. NCAPG2 facilitates glioblastoma cells' malignancy and xenograft tumor growth via HBO1 activation by phosphorylation. Cell Tissue Res 2021; 383: 693–706. https://doi.org/10.1007/s00441-020-03281-y

[21] MENG F, ZHANG S, SONG R, LIU Y, WANG J et al. NCAPG2 overexpression promotes hepatocellular carcinoma proliferation and metastasis through activating the STAT3 and NF-κB/miR-188-3p pathways. EBioMedicine 2019; 44: 237-249. https://doi.org/10.1016/j.ebiom.2019.05.053

[22] BOREL F, KONSTANTINOVA P, JANSEN PLM. Diagnostic and therapeutic potential of miRNA signatures in patients with hepatocellular carcinoma. J Hepatol 2012; 56: 1371-1383. https://doi.org/10.1016/j.jhep.2011.11.026

[23] LI L, GUO Z, WANG J, MAO Y, GAO Q. Serum miR-18a: A Potential Marker for Hepatitis B Virus-Related Hepatocellular Carcinoma Screening. Dig Dis Sci 2012; 57: 2910-2916. https://doi.org/10.1007/s10620-012-2317-y

[24] ZHOU J, YU L, GAO X, HU J, WANG J et al. Plasma MicroRNA Panel to Diagnose Hepatitis B Virus–Related Hepatocellular Carcinoma. J Clin Oncol 2011; 29: 4781-4788. https://doi.org/10.1200/JCO.2011.38.2697

[25] GOTO Y, KUROZUMI A, ARAI T, NOHATA N, KOJIMA S et al. Impact of novel miR-145-3p regulatory networks on survival in patients with castration-resistant prostate cancer. Br J Cancer 2017; 117: 409-420. https://doi.org/10.1038/bjc.2017.19

[26] LIANG ML, HSIEH TH, NG KH, TSAI YN, TSAI CF et al. Downregulation of miR-137 and miR-6500-3p promotes cell proliferation in pediatric high-grade gliomas. Oncotarget 2016; 7: 19723-19737. https://doi.org/10.18632/oncotarget.7736

[27] YAMADA Y, ARAI T, KOJIMA S, SUGAWARA S, KATO M et al. Regulation of antitumor miR-144-5p targets oncogenes: Direct regulation of syndecan-3 and its clinical significance. Cancer Sci 2018; 109: 2919-2936. https://doi.org/10.1111/cas.13722

[28] SARATHI A, PALANIAPPAN A. Novel significant stage-specific differentially expressed genes in hepatocellular carcinoma. BMC Cancer 2019; 19: 663. https://doi.org/10.1186/s12885-019-5838-3